OPTIMIZED SYNTHESIS OF A NANOSTRUCTURED AL ALLOY MODIFIED WITH Cu BY MECHANICAL ALLOYING – *MICROSTRUCTUREAND SOLUBILITY MODELLING PERSPECTIVE*

A. MOLINA-OCAMPO[b], R. A. RODRÍGUEZ-DÍAZ[a,b*], A. SEDANO[b], S. SERNA[b], J. PORCAYO-CALDERÓN[b], J. JUAREZ-ISLAS[c], S. GAONA-JIMÉNEZ[a]

[a]*Universidad Politécnica del Estado de Morelos, Boulevard Cuauhnahuac 566, Col. Lomas del Texcal, 62574 Jiutepéc, Morelos México*

[b]*Centro de Investigación en Ingeniería y Ciencias Aplicadas, UAEM, Av. Universidad 1001, Col, Chamilpa, Cuernavaca Mor., México.*

[c]*Instituto de Investigaciones en Materiales-UNAM, circuito exterior S/N, Ciudad Universitaria, C. P. 04510, México DF, México.*

In the present investigation, a nanostructured solid solution of Cu dissolved in Al was elaborated by mechanical alloying MA technique, from a stoichiometric mixture of high purity powders of Cu and Al. The particle size of powder mixture diminished from 2.8 μm to 1.4 μm while the process time had elapsed from 2.5 h to 20 h. According to the X-ray diffraction analysis, a solid solution of Cu in Al (α-Al) had begun to form at the early stage of process (2.5 h) and continued to the end of ball milling. The size of nanometric grains that belongs to the nanostructured solid solution (α-Al), was diminished from 33.9 nm to 27.7 nm while the milling time had elapsed from 2.5 h to 20 h; similarly, the nanometric-sized grains decreased slightly when the milling time had advanced from 15 h to 20 h. This trend pointed toward achieving the minimum or optimal crystallite size.

(Received March 23, 2016; Accepted May 30, 2016)

Keywords: Al alloy, Ball milling, Mechanical alloying, Microstructural characterization, Solid solution, Nanostructured alloy

1. Introduction

Mechanical Alloying (MA) is a non-equilibrium processing technique that has been developed in the last decades and has found a great number of applications in order to obtain materials with a more refined microstructure and enhanced properties. Examples of materials obtained by MA include oxide-dispersion strengthened (ODS) nickel-base superalloys, amorphous materials, metallic glasses, quasicrystals, intermetallic compounds, nanocrystalline materials, high-temperature superconductors, materials for hydrogen storage, and so on [1].

MA is a solid-state powder processing method which permits the production of homogeneous materials, from a mixture of metallic or ceramic powders [2, 3]. MA process begins mixing elemental powders inside the milling vial which contains the milling balls, before the milling process begins, the vials are sealed under an inert atmosphere.

After, the powder particles are subjected to high energetic impacts by the balls that collide with one another during the milling process, and the particles undergo deformation, welding or fracture repeatedly [4, 5]. In comparison with the conventional route of solidification, mechanical alloying is a low cost and simpler technique to produce nanostructured alloys. This processing technique allows to produce the alloying of constituent elements with different melting points or those that are immiscible in the solid state, which is often difficult or impossible by conventional solidification techniques. In addition, the mechanically alloying process can produce solid solutions with extended solid solubility limits observed under equilibrium processing. MA or ball

*Corresponding author: rdiaz.unam@gmail.com

milling is capable to synthetize stable and metastable solid solutions from a mixture of metallic or ceramic powders [1]. However; systematic studies have not been conducted on the variation of solid solubility limits with the different process parameters.

The solid solubility extent can be evaluated and quantified using the X-ray diffraction technique (XRD), generally from changes in the reticular constant values computed from the shift of the positions of the diffraction peaks, or even the absence of peaks corresponding in this case to the solute element. Generally, the absence of second phase reflections in the X-ray diffraction profiles has been associated to the absence of second phases, and hence the formation of a homogeneous solid solution. However, both these conclusions deal with various problems and so the values reported may not always be accurate. Therefore, for a more accurate estimation of the solid solubility levels and extension, it is necessary to use more than one characterization technique [6]. The Al-Cu binary alloy system is of particular interest [7], due to the fact that the Al-rich Al–Cu alloys provide age-hardening and oxide-dispersion strengthening mechanisms once the appropriate thermal treatment is applied in order to develop superior mechanical properties, while the Cu-rich Cu–Al alloys exhibit excellent corrosion resistance, and also thermal, mechanical and electrical properties.

Previous investigations of mechanical alloying of Al and Cu powders [8, 9] showed that it is possible to produce solid solutions or intermetallic phases at low temperatures.

Similar to multi-pass cold rolling, the ball milling technique is capable to produce an Al/Cu composite structure in each of the powder particles [10, 11], which is generated by the repeated collisions of balls with the metallic particles. This composite structure can be considered as a stack of a great number of Al/Cu diffusion couples. Once, the composite structure is formed, the advance of milling process induces a refinement of the composite structure and under certain conditions solid state reactions between Al and Cu could be activated [12].

Thus, the purpose of this research is to study the effect of the parameters of processing of MA on the production of solid solutions of Cu solute in Al matrix with optimized microstructural properties.

2. Experimental

Elemental powders of Al and Cu (99.9 % purity)) were blended in stoichiometric ratio to yield Al-3Cu (wt.%). The mixture was poured in a hardened steel vial with balls of the same material. Analytical grade methyl alcohol, as process control agent (PCA), was added in a ratio of 0.003 ml by gram of mixture. Subsequently, the mixture was put inside the hardened steel vial under an argon atmosphere and its screw cap was closed. Finally in this way, the mixture was ball milled by using a planetary mill at the speed of 300 RPM during different milling times: 2.5, 5, 7.5, 10, 15 and 20 h. During the mechanical milling experiments, a balls-to-powder weight ratio of 10: 1 was employed.

Morphological evolution, particle size, and chemical homogenization of the powder mixture was characterized in a scanning electron microscope (SEM) mark Estereoscan 440 connected to a Si detector with window of Be (mark Oxford Pentafel) with a resolution of 163 eV which was attached to a software of energy dispersive spectroscopy (EDS), this with the purpose to perform chemical microanalyses. SEM technique was also utilized to carry out punctual chemical analysis in the un-milled and processed samples. X-Ray Diffraction technique was employed to determine and identify the crystalline structure of the different phases formed during milling, also to determine the crystallite size and lattice parameter from X-ray diffraction peaks. To perform this analysis, it was utilized a Siemens Diffractometer D500, in which a voltage of 30kV was employed and a current of 20 mA. The specimens were scanned with a filter of CuKα radiation with a wavelength of $\lambda = 1.5418$ Å and using a step of 0.020°/0.6 sec., in a range of 30° to 100°.Vegard's law was utilized to study the dependence of the solid solubility variation of Cu in Al with the lattice parameters.

3. Results and discussion

Figure 1 a) and b) displays the elemental powders which corresponds to Al and Cu respectively. Figure 1 a) shows spherical particles (with a mean particle size of 3.81 microns), and smaller particles than 3.81 microns, belonging to Al. Figure 1 b) shows that the Cu particles possess a dendritic-type morphology with an average size of dendritic arm of 2.68 microns and a total particle size of 75 microns.

Figure 2 shows the variation of the particle size and morphology with milling time when the powder mixture was milled at 300 RPM. This illustration displays particles located on surface of agglomerates.

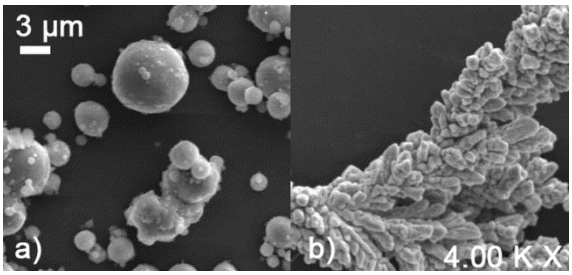

Fig. 1. Scanning electron micrograph of a) particles of Al and b) particles of Cu, both micrographs were obtained at 4000x.

Figure 3 shows the statistic variation of the particle size as a function of milling time. In this plot, the most important values plotted in each box are the minimum and maximum values and the average value (the circle inside the box). This graph shows that the average value of particles diminished from 2.6 to 1.33 µm while the milling time had elapsed from 2.5 to 20 h. However at the early stage of milling of 2.5 h, the powder mixture possessed the biggest particle size distribution, with values ranging from 1.1 to 5.5 µm. This behavior could be attributed to the diminution of the size of the copper particles and the size decrease of the aluminum particles. In this case, the mean particle size of the powder mixture (2.65 µm) had decreased in relation with the initial average size of the Al particles. As the milling time advanced from 2.5 to 5 and 15 h, the interval of particle size distribution had decreased simultaneously as the average particle size had diminished. This behavior is due to the hardening of the particles induced by the mechanical working produced by the continuous mechanical energy provided by the repeated collisions of the balls with the powder particles which in turn had generated a fracture process by a fatigue failure mechanism and / or by the fragmentation of fragile flakes simultaneously with the advance of milling time. At this stage of milling, the tendency to fracture of the particles prevails over the cold welding.

Figure 3 also exhibits that the average particle size diminished insignificantly from 1.5 to 1.3 µm while the milling time had elapsed from 15 to 20 h, this is because after a certain process time, an equilibrium of stable state is reached when a balance has been attained by the welding speed, which tends to enlarge the average particle size with the speed of fracture, which tends to reduce the average size of the composite particle. The smallest particles are capable to experience deformation without fracturing and tend to weld to each other to form larger particles, with an overall tendency to lead fine particles and large particles to an intermediate size.

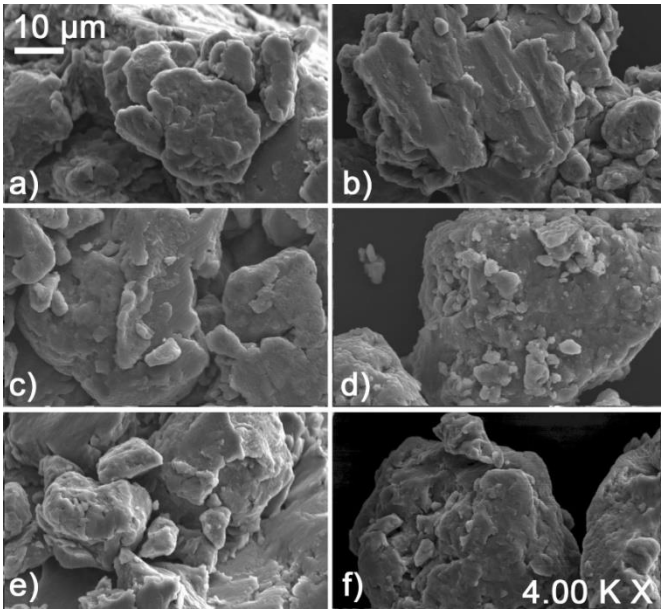

Fig. 2. Microstructural evolution of the mixture of powders of Al-3Cu composition (wt. %) in function of the milling time. (a) 2.5 h, (b) 5 h, (c) 7.5 h, (d) 10 h, (e) 15 h and (f) 20h.

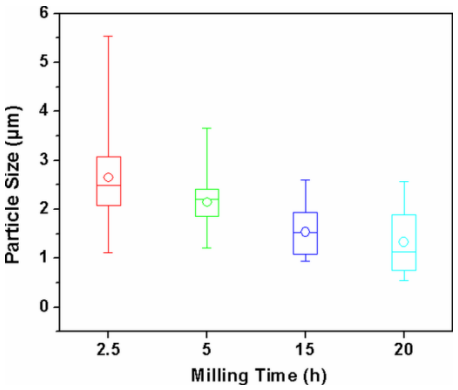

Fig. 3 Variation of the particle size of the powder mixture of Al-3Cu (wt. %) with the milling time. In this case, the powders were milled at 300 RPM.

3.2 Microstructural characterization by X-ray diffraction technique.

Figure 4 shows the X-ray diffraction patterns of the powder mixture Al-3Cu which was ball milled at 300 RPM at different ball milling times.

The X-ray diffraction profiles of the mixture of powders in the un-milled condition are displayed in Figure 4 (a), where the peaks corresponding to the elemental powders Al and Cu are exhibited. According to this figure, the diffraction peaks corresponding to pure Cu decreased in intensity from the beginning of milling process and disappeared at the tenth hour of milling, this finding could be attributed to the continuous solubilization process from the beginning to the end of milling. Only the diffraction peaks belonging to the solid solution labeled as α-Al can be observed after de tenth hour of ball milling process. According to the binary alloy Cu-Al phase diagram [13] the equilibrium solid solubility of Cu in Al at room temperature is only 0.02 at. % Cu [14]; however an extension of the solid solubility from 0.02 at. % to 2.7 at. % of Cu in Al has been attained by employing the mechanical alloying technique in previous researches [15]. Besides, the width of diffraction peaks at half its height belonging to the solid solution α-Al experienced a broadening as the milling time had elapsed. This behavior, as is well known is related to a decrease of crystallite size [16-17].

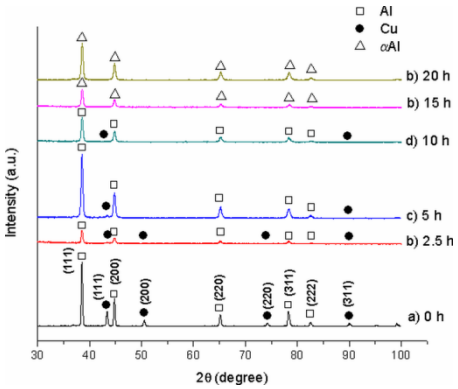

Fig. 4 X-ray diffraction profiles of the powder mixture of Al-3Cu (wt. %) milled at 300 RPM at various milling times: a) 0 h, b) 2.5 h, c) 5 h, d) 10 h, e) 15 h and 20 h).

Figure 5 shows the variation of the crystallite size with the milling time of the Al-3Cu (wt%) alloy which was milled at 300 RPM. In this illustration can be clearly observed a tendency to decrease the nano-scaled grain size simultaneously with the course of the ball milling process. In this case, the crystallite size in nm was determined by the Scherrer equation [16] by using the width of XRD diffraction peak at half its height. When the crystallite sizes obtained from all X-ray diffraction peaks were calculated, then a mean value of crystallite size was computed. In the same illustration can be seen a significant decrease from about 38.5 to 27.5 nm when the powder mixture was milled from 2.5 to 20 h, respectively. However, it is worth noting that during the interval of milling (from 15 to 20 h of milling process) the crystallite size diminished slightly in a more stable way. This behavior could indicate that the obtaining of the minor crystallite size, was just going to occur at about 20 h of milling.

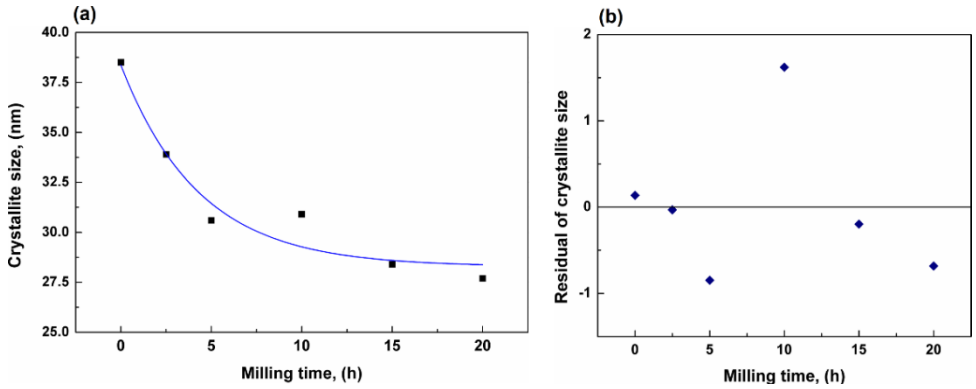

Fig. 5. (a) Crystallite size dependence of the powder mixture of Al-3Cu (wt. %) with the milling time. In this case, the ball milling process was performed at 300 RPM. (b) Residuals plot of crystallite size.

For the values determined for the crystallite size variable, some mathematical models were tested in order to fit and describe the experimental data. The models which were tested are the following: exponential, polynomial, sigmoidal, allometric and multiple regression. The best fitting performance was a decay exponential function and presented a value of 91.91% in the statistical measure for goodness-of-fit, Adj-R square [18]. The specific exponential function is presented in equation 1.

$$L = 28.2852 + 10.0783e^{\left(\frac{-t}{4.3141}\right)} \quad (1)$$

In equation 1, “L” is the crystallite size, and “t” the milling time.

Residuals are independent and unbiased (Garson, 2012), because of their randomness (Figure 5 (b)). Fisher-Test in which the probability $P(F_{value}>F_{table})$ = 2.94306E-5, leads to the conclusion that the relationship between experimental and estimated data is statistically significant [19] .

Figure 6 also shows that lattice strain increased from about 0.08 to 0.55 % when the milling time had elapsed from 0 to 20 h. In this case, it can be affirmed that the increment of lattice strain is produced by the transfer of mechanical energy provided by the repeating impacts of the milling balls to the metallic powders and the subsequent energy storage in form of crystal defects of the element or alloy being milled, where most of this energy is stored in form of vacancies, site-order and/or dislocations. So, in this case, the broadening of diffraction peaks can be due to a significant augment of punctual and linear crystalline defects and a reduction of nano-sized grains with the lapse of milling time. It is worth noting that other sources of strain are the grain boundary triple junction, contact or sinter stresses, stacking faults, coherency stresses, etc. [20]. However; a drastic drop of the lattice strain can be observed when the sample was milled from 5 to 10 h. It can be asseverated that this behavior is due to the accumulation of the great quantity of crystalline defects at the 5^{th} hour of milling and the subsequent stress relief originated by the increment of temperature within the interval of time from 5 to 10 h of milling. Thus, the stress relief is reflected as a reduction of the lattice strain showed in figure 6.

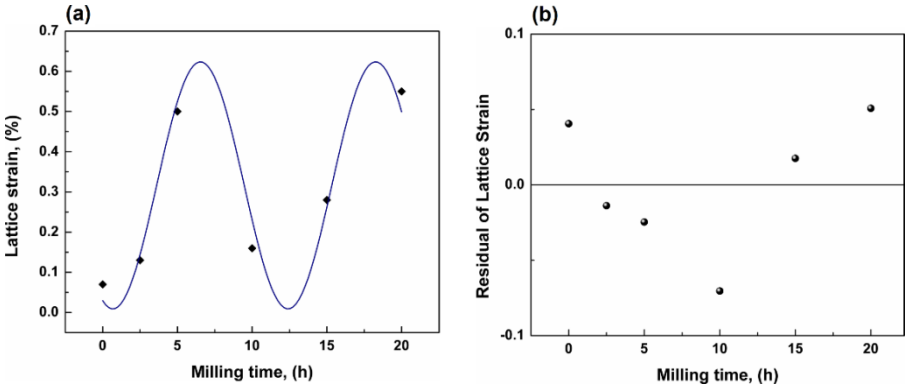

Fig. 6. (a) Lattice strain dependence (nanometric sized grains) of the powder mixture of Al-3Cu (wt. %) with the milling time, (b) Residuals plot of the lattice strain.

With the experimental data obtained for the lattice strain variable,some mathematical models were tested aiming to fit and describe the experimental values. Similarly, the models which were tested are the following: Sine, polynomial, multiple lineal regression and exponential. However; the best fitting performance is a sine function and presented a value of 87.29% in the statistical measure for goodness-of-fit, Adj-R square. The specific sine function is displayed in equation 2.

$$\varepsilon = 0.3164 + 0.3073 \sin\left(\pi\left(\frac{t-3.6122}{5.8585}\right)\right) \quad (2)$$

In equation 2, “ε” is the lattice strain and “t” is the milling time.

Residuals are independent and unbiased (Figure 6 (b)). Fisher-Test in which the probability $P(F_{value}>F_{table})$ = 0.03, leads to the conclusion that the relationship between experimental and estimated data is statistically significant. However, it is worth noting that the sine function describes the behavior of lattice strain in this case only within the interval of milling time “t” 0 h ≤ t ≤ 20 h.

In Figure 7, it can be seen that the lattice parameter underwent a diminution during the time interval of 2.5 to 15 h of milling; however, the lattice constant increased after the 15 h of milling process up to 20 h. The linear decrement of the reticular constant within the interval of

time from 2.5 to 15 h of milling is in agreement with the Vegard´s law which affirms that the lattice parameter of the solvent varies linearly with the variation of the content of solute that is dissolved in the solvent [21-22]. However; the increment of the reticular constant after the 15 h of processing is because the solubilization of Cu within the crystal lattice of Al reached and exceeded its limit of supersaturation. According to figure 8 which represents the Vegard's law, the maximum content of Cu solubilized in Al is 0.8 at. % or 1.84 wt. %. This extent of solid solubility surpass the solid solubility of Cu in Al at room temperature under equilibrium solidification conditions.
With the values computed for the lattice parameter variable, various mathematical models were tested in order to fit and describe the experimental data. The models which were tested are the following: exponential, polynomial and linear.
The best fitting quality for lattice parameter data was of 77.94%, through the linear function displayed in equation 3.

$$a = 4.0508 - 0.00079t \tag{3}$$

In equation 3, "a" is the lattice parameter and "t" is the milling time.

In this case, the residuals are independent and unbiased. Fisher-Test in which the probability $P(F_{value}>F_{table}) = 0.03011$ is statistically significant.

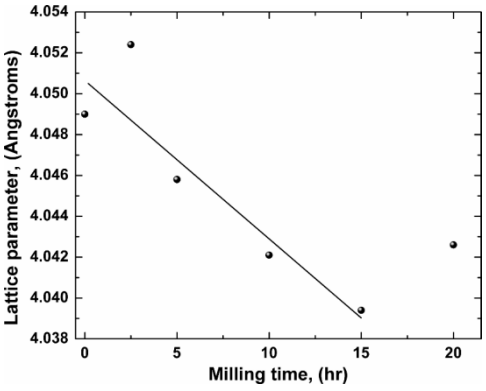

Fig. 7 Variation of the size of the lattice parameter of the powder mixture of composition Al-3Cu (wt. %) based on the milling time.

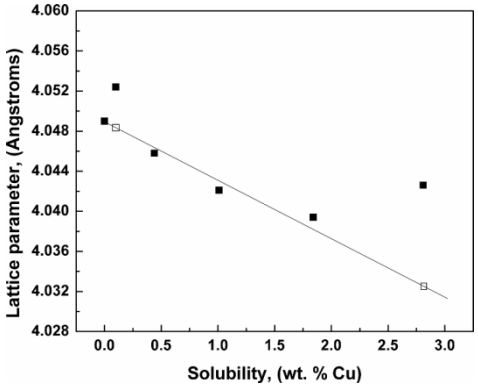

Fig. 8 Lattice parameter of pure Al and the Al-Cu solid solution as a function of Cu concentration.

Fig. 8 shows theVegard´s law plot computed from the reticular parameters obtained by using the experimental results. From this illustration, it can be observed that the lattice constant of pure Al or the solid solution Al-Cu varies predominantly in a linear way from 0 to 15 h of milling with exception of the sample milled during 2.5 h. In this case, the physical origin of the deviations of the lattice constants from Vegard's law could be mainly due to the large size mismatch between

the solute and the solvent atoms. This behavior, can also be due to the formation of nonrandom alloys which is related in this case with the clustering of Cu, since Vegard's law would be strictly valid only if the Cu atoms would be statistically randomly distributed in the solid solution formation process [23]. This asseveration is valid and rational since during the first 2.5 h of milling the process of solid solubilization of Cu in Al had begun, but at this stage the Cu was not still uniformly distributed in the Al matrix or solvent. Another explanation why the lattice constant was deviated from vegard's law, is because the milling of the sample during 2.5 h induced a lattice strain generated by the cold working provided during the first stage of process.

The solid solubility of Cu in Al as a function of milling time is showed in Figure 9, this illustration shows a continuous increment of solid solubility of Cu in Al from 0 to 1.8 wt% Cu while the milling time had advanced from 0 to 15 h of milling. This comportment is obviously due to the inter-diffusion that had occurred between the components as a result of the mechanical alloying process. It is worth noting that the solid solubility value of the sample milled during 15 h in present work has already surpassed in a drastic way the solid solubility reported previously at room temperature (0.05 % wt. Cu). In previous researches, solid solubility extensions have been attained in many alloy systems by non-equilibrium processing methods such as RSP [24] and vapor deposition [25]. In the first years of MA investigation, the observation of solid solubility extensions was not the primary research objective; instead, formation of solid solutions was discovered as an alternate result during amorphization of metal powder mixtures.

Figure 9 shows that the solid solubility limit increases with milling time as diffusion progresses; however the solid solubility limit have a tendency to increase without any evidence that the Al-Cu system have reached a (super)saturation level, beyond which no further extension of solid solubility occurs. The reticular constants of the samples milled during 2.5 and 20 h were included in the plot of solid solubility as extrapolated data, since the calculation of the concentration of Cu dissolved in Al would result in erroneous values.

For the experimental data of solid solubility expressed in wt. %, the best fitting performance is an increasing exponential function and presented a value of 99.75% in the statistical measure for goodness-of-fit, Adj-R square. The specific function that describes the experimental data pertaining to the solubility is presented in equation 4.

In equation 4, S_s is the solid solubility and t is the processing time. In this case, the residuals are independent and unbiased (Figure 9 b). Fisher-Test in which the probability $P(F_{value}>F_{table})$ = 3.6044E-5 implies that the relationship between experimental and estimated data is statistically significant.

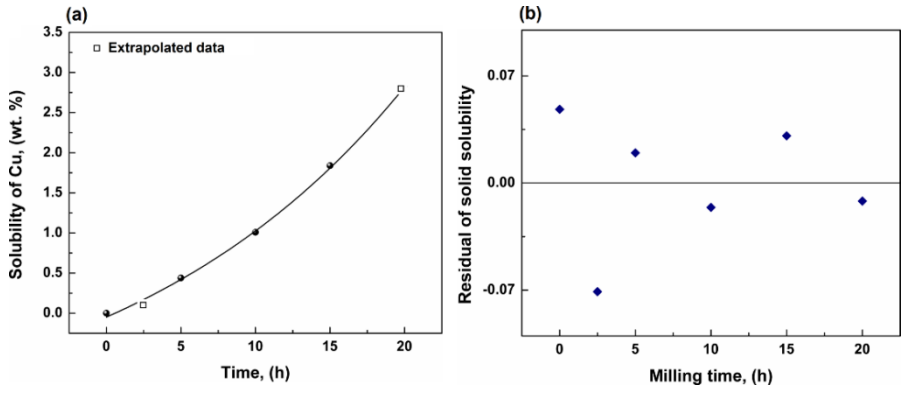

Fig. 9 (a) Solid solubility of Cu in Al as a function of milling time, (b) residuals plot of solid solubility.

4. Conclusions

The particle size was decreased significantly from 2.6 to 1.33 μm while the milling time had advanced from 2.5 to 20 h, however, the particle size diminished insignificantly from 15 to 20 h of process. This behavior observed during the last stage of milling suggest that a balance

between fracture and welding processes among particles was attained, because the size of particles prevailed stable during this interval of milling process.

The crystallite size corresponding to the solid solution of Cu in Al (α-Al) obtained during the mechanical milling process, decreased from 38.5 to 27.5 nm as the milling time had elapsed from 2.5 to 20 h. The crystallite size behavior during the last stage of milling suggested that the minimum crystallite size was about to be reached.

According to the x-ray diffraction analyses, the diminution of the intensity of diffraction peaks corresponding to pure Cu with the advance of milling process could be associated to the continuous solubilization process from the beginning to the tenth hour of milling. However disappearance of the x-ray diffraction peak corresponding to pure Cu could be associated to the complete solubilization of Cu in Al. However, the total disappearance of the Cu peaks in the X-ray diffraction profiles does not indicate that a solid solubility super-saturation level has been attained.

The variation of lattice parameter of the solid solution αAl as a function of the concentration of Cu dissolved in Al matrix, exhibited a linear tendency during the interval of milling from 2.5 h to 15 h. However; after the 15th h of process a deviation from the linear behavior was observed, which means that the Vegard´s law was not fulfilled during the last 5 h of ball milling.

An extended solid solubility was achieved at the 15^{th} h of milling with a value of 1.8 wt. % of Cu.

Acknowledgements

The authors express their gratitude to CONACyT-México for the financial support granted for the development of this research. Also to the technicians Adriana Tejeda and Carlos Flores-Morales for their support in the microstructural characterization of materials.

References

[1] C. Suryanarayana, Progress in Materials Science **46**, 1 (2001).
[2] J. S. Benjamin, Materials Science Forum **88-90**, 1 (1992).
[3] C. Suryanarayana, E. Ivanov, V. V. Boldyrev, Materials Science and Engineering A **304-306**, 151 (2001).
[4] J. S. Benjamin, T. E. Volin, Metallurgical Transactions **5**, 1929 (1974).
[5] P. S. Gilman & W. D. Nix, Metallurgical Transactions A **12**(5), 813 (1981).
[6] R. A. Rodríguez Díaz, A. Molina Ocampo, J. Porcayo-Calderón& J. Juárez Islas, Digest Journal of Nanomaterials and Biostructures **10**, 712 (2015).
[7] H. Baker, Introduction to Alloy Phase Diagrams. ASM International, Materials Park, Ohio (1992).
[8] F. Li, K. N. Ishihara & P. H. Shingu, Metallurgical Transactions A **22A**, 2849 (1991).
[9] S. Xi, J. Zhou, J, Zhang & X. Wang, Journal of Materials Science Letters **26**, 245 (1996).
[10] T. Shanmugasundaram, M. Heilmaier, B. S. Murty& V. S. Sarma, Materials Science and Engineering A **527**, 7821 (2010).
[11] B. J. Aikin& T. H. Courtney, Metallurgical Transactions A **24**, 647 (1993).
[12] D. Y. Ying, D. L. Zhang, Journal of Alloys and Compounds **311**, 275 (2000).
[13] T. B. Massalski, Journal of Phase Equilibria **1**, 27 (1980).
[14] L. F. Mondolfo, (1976) Aluminum alloys: structure and properties. Butterworths, Michigan University (1976).
[15] F. Li, K. N. Ishihara & P. H. Shingu, (1991), Metallurgical Transactions **A22**, 2849 (1991).
[16] P. Scherrer, Mathematisch-physikalischeKlasse **26**, 98 (1918).
[17] J. I. Langford, A. J. Wilson, Journal of Applied Crystallography **11**, 102 (1978).
[18] G. D. Garson, Curve Fitting & Nonlinear regression. Statistical Associates Publishing Blue Book series, North Carolina State University (2012).
[19] G. D. Garson, Testing Statistical Assumptions. Statistical Associates Publishing Blue Book

series, North Carolina State University (2012).
[20] T. Ungar, Journal of Materials Science **42**, 1584 (2007).
[21] L. Vegard, ZeitschriftfürPhysik A Hadrons and Nuclei **5**, 17 (1921).
[22] L. Vegard, ZeitschriftfürKristallographie **67**, 239 (1928).
[23] W. Li, M. Pessa& J. Likonen, Applied Physics Letters **78**, 2864 (2001).
[24] T. R. Anantharaman, C. Suryanarayana, (1971) Journal of Materials Science **6**, 1111 (1971).
[25] C. Suryanarayana (1999) Non-equilibrium processing of materials. Pergamon Press, Oxford, UK, (1999).